information

MDPI

Article

DOA Estimation Algorithm for Reconfigurable Intelligent Surface Co-Prime Linear Array Based on Multiple Signal Classification Approach

Tianyu Lan [1], Kaizhi Huang [1,*], Liang Jin [1], Xiaoming Xu [1], Xiaoli Sun [1] and Zhou Zhong [1,2]

1 PLA Strategic Support Force, PLA Information Engineering University, Zhengzhou 450001, China; no2233t@alumni.sjtu.edu.cn (T.L.); jl@mail.ndsc.com.cn (L.J.); xuxiaomingndsc@outlook.com (X.X.); sunxiaolindsc@outlook.com (X.S.); zhongzhoundsc123@outlook.com (Z.Z.)

2 Purple Mountain Laboratory, Nanjing 211111, China

* Correspondence: huangkaizhi@tsinghua.org.cn

Abstract: Co-prime linear arrays (CLAs) provide an additional degree of freedom (DOF) with a limited number of physical sensors, and thus help to improve the resolution of direction of arrival (DOA) estimation algorithms. However, the DOF of traditional CLA is restrained by the structure of the array, which cannot be adjusted after deployment. In this paper, we propose a DOA estimation algorithm for reconfigurable intelligent surface co-prime linear array (RIS CLA) based on the multiple signal classification approach. Specifically, an RIS CLA is first constructed on the ground of RIS antenna, by turning on/off specific elements at different times. Then, the covariance matrix of the received signal is vectorized, so as to construct a virtual difference array, whose aperture is considerably expanded. Finally, a spectral peak search on the noise subspace of the received signal of the difference array is conducted to obtain the DOA estimation result. Simulations verify the improvement of the proposed algorithm in terms of DOF and resolution. To be specific, the DOF provided by RIS CLA outnumbers that of CLA by more than 30%, and the resolution of the proposed DOA estimation algorithm is effectively improved, with its accuracy increased up to 70% under the low signal-noise-ratio (SNR) scenario, compared with existing algorithms.

Keywords: DOA estimation; reconfigurable intelligent surface; co-prime array; multiple signal classification

Citation: Lan, T.; Huang, K.; Jin, L.; Xu, X.; Sun, X.; Zhong, Z. DOA Estimation Algorithm for Reconfigurable Intelligent Surface Co-Prime Linear Array Based on Multiple Signal Classification Approach. *Information* **2022**, *13*, 72. https://doi.org/10.3390/info13020072

Academic Editor: Kostas Vergidis

Received: 2 January 2022
Accepted: 27 January 2022
Published: 3 February 2022

1. Introduction

Direction of arrival (DOA) estimation [1,2] is a fundamental technique in the field of wireless environment sensing. According to the spatial information provided by DOA estimation, participants of the wireless communication will be able to send and receive signals selectively in the presence of interference, thus increasing system capacity and the effectiveness of spectrum resource utilization. Under the rapid development of 5G/B5G technology, where the spatial spectrum resources will become increasingly scarce, novel approaches for high-resolution DOA estimation are becoming more and more critical.

By far, much research has been conducted to solve the DOA estimation problem [3–19], among which the modified multiple signal classification (MUSIC) algorithm based on co-prime linear array (CLA) [10–19] is considered a high-performance technique. A CLA is composed of two uniform linear arrays (ULAs) as subarrays, and provides a much larger degree of freedom (DOF) than ULAs with the same number of physical sensors, which means that CLA is capable of sensing the incident signals more accurately. However, there are two unsolved problems: (1) a CLA does not guarantee the consecutiveness of the difference array, which means that there exist some positions where no nominal sensors exist in its difference array, and the resolution of DOA estimation is affected; (2) it is unlikely to adjust the structure of a deployed CLA as frequently as is needed, once it is deployed. These problems are ultimately caused by the non-adjustability of traditional arrays. Therefore, novel designs that are able to adjust the structure of the array are expected to solve the problems.

Against this background, reconfigurable intelligent surface [20–22] antenna array (RIS array), based on digital metamaterial [23,24], is an exciting and promising technique. Composed of numerous real-time-controllable digital metamaterial units, an RIS array is capable of adjusting the electromagnetic characteristics of the units whenever necessary. Dai et al. proposed for the first time the design of the RIS-based antenna array design and further provided experimental data on its performance in [25]. Although related research is still in its infancy, RIS array is still one of the most promising techniques for overcoming the defects of traditional CLA, whose array geometry is fixed and uncontrollable. Furthermore, RIS array provides brand new possibilities, from implementation to characteristics control of antenna arrays with high controllability and geometrical redundancy, and is therefore a promising way to perform high-resolution DOA estimation.

In this paper, a DOA estimation algorithm of RIS CLA is proposed for the very first time. The main contributions are as follows:

- We proposed a layout of DAC module in an RIS array, so as to convert RIS array into an equivalent ULA. Then we introduce the concept of RIS CLA, which consists of RIS-based CLAs, and proposed a method to implement RIS CLA via controller.
- We proposed the signal receiving model of RIS CLA, based on its agile characteristics to change the configuration of subarrays.
- On the grounds of the model above, we, for the very first time, introduce a signal preprocessing method before MUSIC-based DOA estimation is conducted. During the preprocessing, the covariance matrix of the received signal is vectorized so as to construct a virtual difference array with higher DOF.
- To verify the feasibility as well as the resolution of the proposed algorithm, several simulative experiments were conducted. Results show that the DOF of RIS CLA improved by more than 30% compared with the traditional CLA. Moreover, the proposed algorithm can distinguish multiple irrelevant incident signals effectively. In terms of resolution, the accuracy of the proposed algorithm exceeds that of the traditional MUSIC algorithm by more than 70%, and is even 30% better than that of the MUSIC algorithm based on traditional CLA, under low SNR scenario.

The rest of this paper is organized as follows: Section 2 introduces the related works. The signal model of CLA and the basic process of DOA estimation are explained in Section 3. In Section 4, a DOA estimation algorithm for RIS CLA based on MUSIC is proposed. Section 5 provides the simulation result of the proposed algorithm, which is later analyzed and discussed. Section 6 summarizes the paper and puts forward several possible research directions in the future.

2. Related Works

Research regarding the DOA estimation problem can be categorized into two major groups. The first one is based on traditional uniform linear arrays (ULAs) and aims to design the algorithm with which the received signal is processed to obtain the DOA information. Schmidt proposed the classic MUSIC algorithm in [3]. By dividing signal subspace and noise subspace, MUSIC achieves super-resolution but the complexity is rather high, and it does not perform well dealing with coherent signals. To tackle the problems, Rao et al. proposed root-MUSIC [4] and reduced the complexity of MUSIC while maintaining the resolution. The spatial smoothing MUSIC algorithm (ss-MUSIC) is introduced in [5], which can estimate the DOA of coherent signals at the cost of the resolution. Furthermore, weighted MUSIC (w-MUSIC) is introduced in [6], which reveals the relationship between MUSIC and other DOA estimation algorithms such as minimum variance method (MVM) [7] and maximum entropy method (MEM) [8]. Other algorithms, such as estimating signal parameters via rotational invariance technique (ESPRIT) and its extended algorithms [9–11] also perform well. To summarize, this kind of research focuses on how the received signal is processed, and is based on the traditional ULA [12].

However, it is neither applicable nor unacceptable to increase the DOF of the ULA, which is the number of sensors, merely by deploying more sensors. Hence, some researchers concentrated on the design of the geometry of the array, attempting to increase the DOF of the array. Co-prime linear array (CLA) is one of the promising techniques therein [13–19]. A CLA, first proposed in [13] by Pal et al., consists of two ULAs acting as two subarrays with the number of sensors co-prime to each other. Compared with ULAs with the same number of physical sensors, CLA provides additional DOF without deploying more sensors, since the array structure is skillfully designed to form a virtual array known as a difference array. Consequently, resolution of DOA estimation algorithms based on CLA improved as well. Pal et al. further proposed augmented co-prime linear arrays [14], a better geometry which further improves DOF of the array, together with the resolution of the DOA estimation algorithm. In [15], two operations with which the CLA can be generalized are proposed. Jia et al. introduced a DOA estimation algorithm for coherent and incoherent sources based on co-prime array in [16], and Dong et al. came up with a method to estimate DOA in the presence of impulsive noise [17]. Furthermore, a proximal gradient-based approach is introduced in [18] to improve the resolution, while Ashok et al. proposed in [19] a low-complexity DOA estimation method on the basis of unfolded CLAs.

3. DOA Estimation Based on Traditional CLA

Based on the sparse structure of physical sensors, CLAs improve the DOF of the array effectively, by designing the arrangement of its elements. Consequently, DOA estimation algorithms based on CLA have improved greatly in terms of resolution compared with those based on ULA.

3.1. Typical CLA Structure

A typical CLA consists of two ULA subarrays with co-prime numbers of sensors, as is shown in Figure 1, with the space between the elements $b{\cdot}d$ and $a{\cdot}d$, respectively (d is half wavelength). Both subarrays take the sensor on the far left as the reference point.

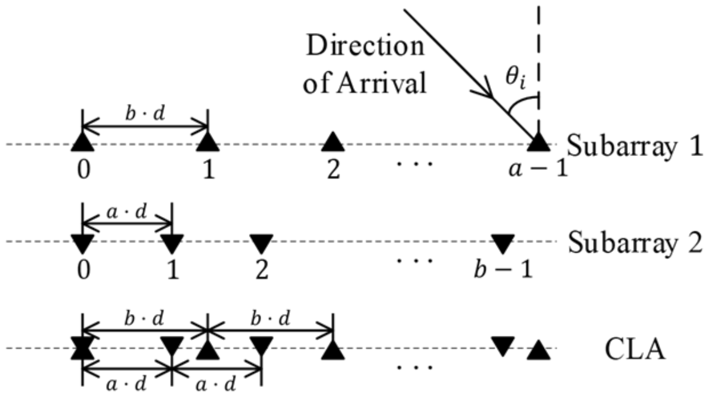

Figure 1. Structure of a typical CLA.

Accordingly, a virtual array called a difference array can be constructed, in which the position of the nominal sensors is given by a linear difference operation on the sensor position of the subarrays. The location set L of the CLA in Figure 1 can be expressed as follows:

$$L = \{\pm(ak_1 d - bk_2 d) | 0 \le k_1 \le b-1,\ 0 \le k_2 \le a-1\}, \tag{1}$$

It is observed that the difference rearranges the sensors in the subarrays, and the number of nominal sensors reaches up to $2ab - a - b$, which indicates that a CLA can provide a DOF of $O(AB)$ with $(a+b-1)$ physical sensors.

For example, for a CLA, whose subarrays contain three and five sensors respectively, the distribution of the nominal sensors in the corresponding difference array is shown in Figure 2, where the black dot represents the presence of a nominal sensor at the position and the white dot means no nominal sensors exist at the position. It is clear that its DOF reaches 21, even though there are only seven physical sensors deployed. However, the elements are not continuously distributed in the difference array, which is the case for most CLA configurations. For this given example, there are no nominal sensors at the position of ± 8 and ± 11; the DOF, therefore, is affected.

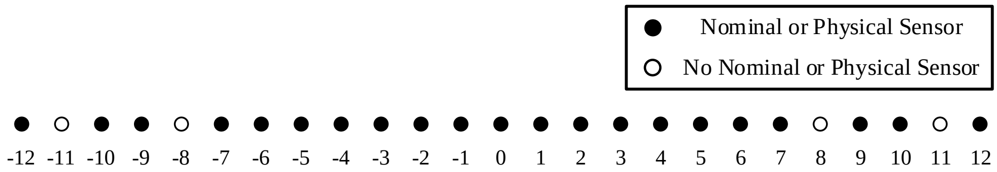

Figure 2. Difference array of a CLA with $a = 3,\ b = 5$.

3.2. DOA Estimation Algorithm of CLA Based on MUSIC Method

Suppose there is a system composed of a CLA that has two subarrays with a and b sensors and K impinging incoherent far-field narrowband signals of power $\boldsymbol{\sigma} = \{\sigma_1^2, \sigma_2^2, \ldots, \sigma_K^2\}$ and incident angle $\boldsymbol{\theta} = (\theta_1,\ \theta_2,\ \ldots, \theta_K)$, respectively.

The signal received by the CLA, denoted by $\boldsymbol{x}(t)$, at a given timeslot t can be expressed as follows, where $\boldsymbol{s}(t)$ and $\boldsymbol{n}(t)$ represent the signal vector and additive white Gaussian noise (AWGN) with average value 0 and power σ_n^2, respectively.

$$\boldsymbol{x}(t) = \boldsymbol{A_c}\boldsymbol{s}(t) + \boldsymbol{n}(t) = \sum_{k=1}^{K} \boldsymbol{a}(\theta_k) s_k(t) + \boldsymbol{n}(t) \tag{2}$$

The array manifold matrix of the given CLA is then given by:

$$\boldsymbol{A_c} = [\boldsymbol{a_c}(\theta_1), \boldsymbol{a_c}(\theta_2), \ldots, \boldsymbol{a_c}(\theta_K)], \tag{3}$$

where $\boldsymbol{a_c}(\theta_k) = \left[\boldsymbol{a_1}^T(\theta_k),\ \boldsymbol{a_2}^T(\theta_k)\right]^T$, $\boldsymbol{a_1}(\theta_k)$, $\boldsymbol{a_2}(\theta_k)$ represents the steering vector of this CLA, subarray 1 and subarray 2 on direction θ_k. And we have:

$$\boldsymbol{a_1}(\theta_k) = \left[1,\ e^{-\frac{j2\pi b d sin\theta_k}{\lambda}},\ \ldots, e^{-\frac{j2\pi(a-1) b d sin\theta_k}{\lambda}}\right]^T, \tag{4}$$

$$\boldsymbol{a_2}(\theta_k) = \left[1,\ e^{-\frac{j2\pi a d sin\theta_k}{\lambda}},\ \ldots, e^{-\frac{j2\pi(b-1) a d sin\theta_k}{\lambda}}\right]^T \tag{5}$$

During the DOA estimation, the observed values of the covariance matrixes of the two subarrays are obtained according to signals received within J snapshots. Then the eigenvalue decomposition of the matrixes is performed, respectively. With the eigenvalues ranked in descending order, the signal subspace and noise subspace are divided, followed by the spectral peak search in the noise subspace for each subarray. Eventually, the estimation results are compared and the final result of DOA estimation is given accordingly.

The advantages of CLA can be summarized as follows: Firstly, the arrangement of sensors of CLA realizes the sub-Nyquist sampling rates [26], which helps to reduce estimation error caused by the mutual coupling effect between sensors. Secondly, the DOF of CLA is generally much greater than that of traditional ULAs, as is illustrated in Figure 2.

Although traditional CLAs help to improve the DOF through the design of sensor arrangement, there are some defects as well. On the issue of DOA estimation, the discontinuous location distribution of sensors in the difference array, as mentioned in Section 3.1, is the main problem. While certain DOA estimation algorithms that require a continuous array may be unsuitable for CLA, it also affects the DOF and hence limits the resolution of DOA estimation. On the other hand, for traditional CLAs, its DOF cannot be improved by means of changing the way the sensors are arranged. RIS technique, which enables real-time controllability of arrays, can effectively solve this problem. Therefore, this paper proposes a DOA estimation algorithm of RIS CLA based on MUSIC method, where RIS technique is used to switch between different CLA configurations, so as to provide higher DOF. Then, based on the idea of MUSIC algorithm, DOA estimation is performed, which further improves the resolution.

4. DOA Estimation Algorithm for RIS CLA Based on MUSIC

In order to further improve the estimation resolution, a DOA estimation algorithm for RIS CLA based on MUSIC is proposed. The algorithm consists of two phases. In phase 1, an RIS CLA is constructed based on RIS array, by means of adjusting the on/off state of the elements instantaneously, followed by signal reception. In phase 2, the received signal is preprocessed, where the covariance matrix of the received signal is vectorized so as to construct a virtual difference array, whose DOF is higher. Finally, a spectral peak search is conducted on the noise subspace of the received signal of the difference array to estimate the DOA of different signals.

4.1. RIS CLA

The RIS CLA proposed in this essay is based on the 2-bit RIS antenna array in [22]. Specifically, for an RIS array consisting of $M \times N$ units, the same digital analog converters (DACs) are used to process the signals received by RIS units located in the same column. Thus, the RIS array is, to some extent, equivalent to a ULA with N elements, which is shown in Figure 3.

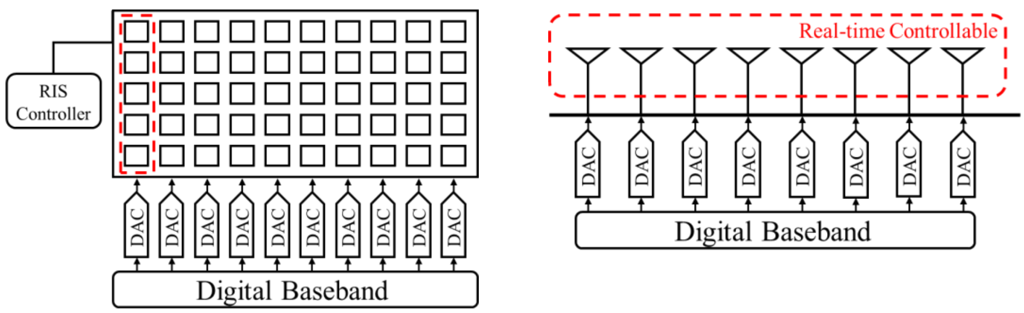

(**a**) (**b**)

Figure 3. Structure of an RIS array: (**a**) layout of DAC module; (**b**) the equivalent model of RIS array.

In particular, since the RIS array is capable of adjusting its elements within a time scale of 10 ns via the controller, this equivalent ULA is endowed with the ability to adjust the array arrangement rapidly. On the other hand, although the RIS array can flexibly change its radiation pattern, DOA estimation based on subarrays with different radiation patterns will greatly reduce DOF of the array. Therefore, the radiation pattern of all subarrays in this essay remains consistent and unchanged.

On the basis of the RIS array, the construction of an RIS CLA is hereby proposed. Specifically, for an RIS array with N columns of elements, if there exist two co-prime numbers, say a and b, that satisfy $N = a{\cdot}b$, then a pair of subarrays of RIS CLA can be constructed by adjusting the RIS array, according to the following method:

Control the RIS array, so that the $l{\cdot}b$-th $(0 \leq l \leq a-1)$ element is turned on, while other elements remain off at time t_1. Denote this subarray with a elements as Subarray 1;

Turn the $l{\cdot}a$-th $(0 \leq l \leq b-1)$ element on, while other elements remain off at time t_2. Denote this subarray with b elements to be Subarray 2.

Since the adjusting process can be conducted within a very short time, it is presumed that the signal received by different subarrays remains the same during the process stated above, in terms of critical parameters like DOA, frequency and transmitting power.

In addition, the RIS CLA can realize multiple CLAs with different configurations, thus providing higher DOF, simply by performing the same method proposed above with different pairs of co-prime numbers.

4.2. DOA Estimation Based on RIS CLA

Since it is capable of constructing CLAs with different combinations of subarrays, RIS CLA provides a higher DOF, which can be utilized to improve the resolution of DOA estimation. However, if the DOA estimation for RIS CLA is conducted following the idea mentioned in Section 3.2, where the estimation is performed separately for each subarray and the final result is obtained by comparing the results, more systematic errors will be introduced, leading to loss of accuracy. Therefore, it is necessary to preprocess the received signal, so that the advantage of a higher DOF can be transformed into more spatial information about the incident angle and a higher resolution of the estimation algorithm. During the preprocessing, the received signals of different subarrays are all considered as the observed value of the received signal of RIS CLA. Then, the difference array is constructed by vectorizing the covariance matrix of the received signal, followed by subspace decomposition and spatial spectral peak search that gives the final DOA estimation result. In this way, the influence of the subarray estimation error can be avoided and the resolution of the final result can be improved.

Specifically, if the received signal of RIS CLA is $\boldsymbol{x}(t)$, its covariance matrix $\boldsymbol{R_x}$ can be expressed as follows:

$$\boldsymbol{R_x} = \boldsymbol{E}\left\{\boldsymbol{x}(t)\boldsymbol{x}^H(t)\right\} = \boldsymbol{E}\left\{\left[\boldsymbol{A_c}(\theta)\boldsymbol{s}(t)\boldsymbol{x}^H(t)\right]\left[\boldsymbol{A_c}(\theta)\boldsymbol{s}(t)\boldsymbol{x}^H(t)\right]^H\right\} = \boldsymbol{A_c}\boldsymbol{R_s}\boldsymbol{A_c}^{\boldsymbol{H}} + \sigma_n^2\boldsymbol{I}_N \quad (6)$$

where $\boldsymbol{R_s}$ and $\boldsymbol{A_c}$ are the eigenvector of the signal subspace and the manifold matrix of the RIS CLA, respectively. Thus, we have:

$$\boldsymbol{A_c} = [\boldsymbol{a}(\theta_1), \boldsymbol{a}(\theta_2) \ldots, \boldsymbol{a}(\theta_K)], \quad (7)$$

where $\boldsymbol{a}(\theta_k)$ represents the steering vector of RIS CLA on direction θ_k, formed by the steering vectors of multiple subarrays on θ_k as shown below (H denotes the number of different subarrays):

$$\boldsymbol{a}(\theta_k) = \left[\boldsymbol{a}_{\boldsymbol{1}}^{\boldsymbol{T}}(\theta_k), \boldsymbol{a}_{\boldsymbol{2}}^{\boldsymbol{T}}(\theta_k), \ldots, \boldsymbol{a}_{\boldsymbol{H}}^{\boldsymbol{T}}(\theta_k)\right]^T, \ 1 \le k \le K \quad (8)$$

Vectorize $\boldsymbol{R_x}$, and we have:

$$\boldsymbol{z} \triangleq vec\{\boldsymbol{R_x}\} = (\boldsymbol{A_c}^* \times \boldsymbol{A_c})\ vec\{\boldsymbol{R_s}\} + \sigma_n^2\ vec\{\boldsymbol{I}_N\} = (\boldsymbol{A_c}^* \times \boldsymbol{A_c})\boldsymbol{p} + \sigma_n^2\boldsymbol{I} \quad (9)$$

where $\boldsymbol{p} = \left[\sigma_1^2, \ \ldots, \sigma_K^2\right]^T$, $\boldsymbol{I} = vec\{\boldsymbol{I}_N\}$, and '×' represents the Kronecker product. Actually, the equation above implies that z behaves as a received signal of an array, whose manifold matrix is $(\boldsymbol{A_c}^* \times \boldsymbol{A_c})$. For convenience we denote a matrix $\boldsymbol{B}$ as follows:

$$\begin{aligned} \boldsymbol{B} &= (\boldsymbol{A_c}^* \cdot \boldsymbol{A_c}) \\ &= [\boldsymbol{a}^*(\theta_1) \times \boldsymbol{a}(\theta_1), \boldsymbol{a}^*(\theta_2) \times \boldsymbol{a}(\theta_2), \ \ldots, \boldsymbol{a}^*(\theta_K) \times \boldsymbol{a}(\theta_K)] \\ &\triangleq [\boldsymbol{b}(\theta_1), \ \boldsymbol{b}(\theta_2), \ldots, \boldsymbol{b}(\theta_K)] \end{aligned} \quad (10)$$

The i-th column of $\boldsymbol{B}$, namely $\boldsymbol{b}\theta_i$, contains phase information which has a one-to-one correspondence with the location of nominal sensors in the RIS CLA.

For example, when $H = 2$, the phase information contained in $\boldsymbol{b}(\theta_i)$ can be expressed as:

$$e^{-\frac{j2\pi(ma-nb)sin\theta_i}{\lambda}}, \ 0 \le n \le a-1, \ 0 \le m \le b-1 \quad (11)$$

The phase information given above is related to the difference array of the CLA, and is identical with that given in (1). We would also like to point out hereby that when $H = 2$, the RIS CLA is actually equivalent to a traditional CLA, under which circumstance its DOF is limited.

When $H > 2$, such correspondence holds as well and the DOF is improved, since more subarrays are constructed. However, there are many repeating rows in $\boldsymbol{z}$ and $\boldsymbol{B}$ after the vectorization in this case, leading to unnecessary increase in algorithm complexity. Therefore, we extract different rows in $\boldsymbol{z}$ and $\boldsymbol{B}$ to reconstruct them as $\widetilde{\boldsymbol{z}}$ and $\widetilde{\boldsymbol{B}}$. The signal reception model can be rewritten as follows:

$$\widetilde{\boldsymbol{z}} = \widetilde{\boldsymbol{B}}\boldsymbol{p} + \sigma_n^2\boldsymbol{I}, \tag{12}$$

Then, decompose the covariance matrix of $\widetilde{\boldsymbol{z}}$ and sort the eigenvalues in ascending order to separate the signal subspace and noise subspace. Finally, search the value of θ corresponding to the spectral peak of function $P(\theta)$, which is given by:

$$P(\theta) = \frac{1}{\boldsymbol{b}^H(\theta)\boldsymbol{E}_{vn}\boldsymbol{E}_{vn}^H\boldsymbol{b}(\theta)}, \tag{13}$$

where $\boldsymbol{E}_{vn}$ is the noise subspace of $\widetilde{\boldsymbol{z}}$, and the set of all results, namely $\hat{\boldsymbol{\theta}}$, is the final estimation result of $\boldsymbol{\theta}$.

Given K, N and several pairs of co-prime numbers (a_i, b_i) that satisfy $a_i{\cdot}b_i \leq N$ as the input, our algorithm can be summarized as follows:

1. Control the RIS array, so that the $l{\cdot}b_1$-th ($0 \leq l \leq a_1 - 1$) element is turned on, while other elements remain off. Denote this subarray as Subarray 1 and take sampling for J snapshots;
2. Control the RIS array, so that the $l{\cdot}a_1$-th ($0 \leq l \leq b_1 - 1$) element is turned on, while other elements remain off. Denote this subarray as Subarray 2 and take sampling for J snapshots;
3. Change a pair of co-prime numbers and repeat steps 1 and 2 for T times;
4. Construct the observation of $\boldsymbol{R_x}$, namely $\hat{\boldsymbol{R}}_{\boldsymbol{x}}$ according to the $2TJ$ received signals;
5. Vectorize $\hat{\boldsymbol{R}}_{\boldsymbol{x}}$, and obtain $\hat{\boldsymbol{z}}$, the observation of $\boldsymbol{z}$;
6. Sort $\hat{\boldsymbol{z}}$ in phase order and remove redundant rows, mark the result as $\widetilde{\boldsymbol{z}}$;
7. Decompose the covariance matrix of $\widetilde{\boldsymbol{z}}$, and obtain the signal subspace $\boldsymbol{E}_{vs}$ and noise subspace $\boldsymbol{E}_{vn}$;
8. Search the spectral peak of $P(\theta)$, and obtain $\hat{\boldsymbol{\theta}}$, the estimation value of $\boldsymbol{\theta}$.

5. Simulation Result

In this section, we use MATLAB to simulate and analyze the performance of the proposed algorithm. The content of the simulation includes the DOFs of different array designs, followed by the effectiveness and the resolution of the proposed algorithm.

5.1. Spatial DOF of Antenna Array

Compared with the traditional DOA estimation algorithm based on ULA, our algorithm can switch between different array configurations merely by adjusting the on/off status of RIS array elements, without deploying any additional sensors. For example, for an RIS array with $N = 24$, the set of different array configurations is shown as follows:

$$(3,8),(2,11),(3,7),(4,5),(2,9),(3,5),(2,7),(3,4),(2,5),(2,3)$$
$$\{(3\ ,\ 8),(2\ ,\ 11)\ ,\ (3\ ,\ 7)\ ,(4\ ,\ 5)\ ,(2\ ,\ 9)\ ,\ (3\ ,\ 5)\ ,(2\ ,\ 7)\ ,(3\ ,\ 4)\ ,(2\ ,\ 5)\ ,(2\ ,\ 3)\}$$

When N increases, the number of array configurations increases as well, which helps to provide higher spatial DOF for RIS CLA. Figure 4 shows the DOF of RIS CLA compared with other array structures when N equals to 30 and 42, respectively. In the comparison group, the subarray combination for CLA in two scenarios is (5, 6) and (6, 7), and the total number of element arrays in the ULA is 10 and 12.

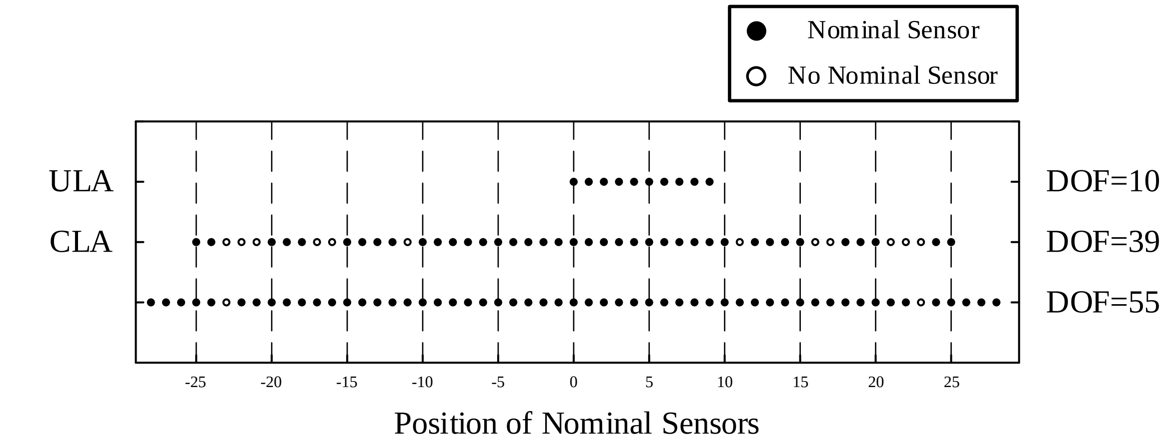

(**a**)

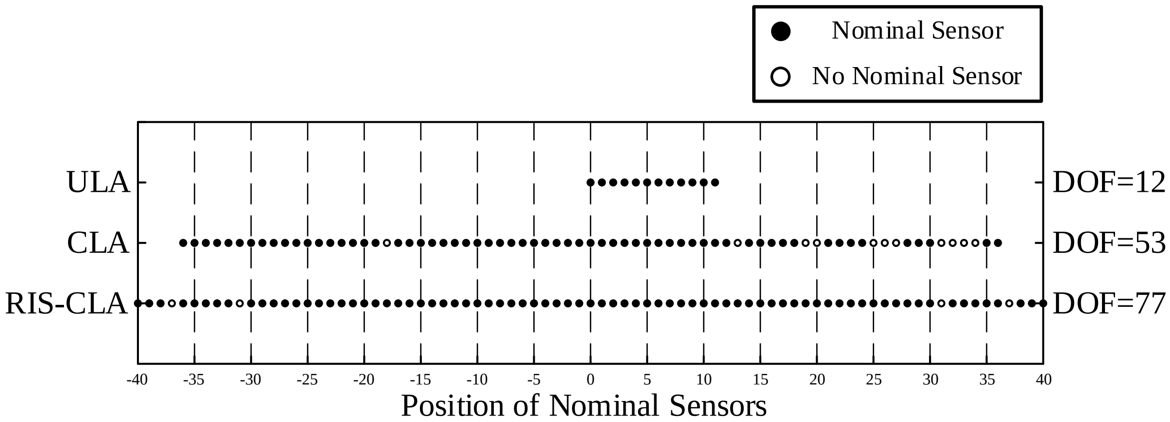

(**b**)

Figure 4. Comparison of DOF of three different arrays: (**a**) $N = 30$; (**b**) $N = 42$.

It is clear in Figure 4 that the DOF provided by RIS CLA array is much greater than that provided by ULA, and is also 35% higher than that of CLA.

5.2. Effectiveness of the Algorithm

Higher DOF means stronger ability to distinguish between different signals. For a highly functional DOA estimation algorithm, it should be able to tell incident signals from the noise, to tell different signals apart and give their incident angles. Therefore, Monte Carlo simulation (MCS) is performed to verify the effectiveness of the proposed algorithm, with $N = 30$.

Firstly, the effectiveness of the algorithm is verified when the number of signals is limited. For the first scenario, there are $K = 7$ incoherent narrowband incident signals, uniformly distributed between $[-\pi/4, \pi/4]$, with the SNR 10 dB. The sampling snapshots of each subarray are $J = 100$, and the number of cycles, which is the number of array configurations used, is $t = 4$. For this scenario, the number of incident signals is smaller than any possible number of physical sensors turned on by RIS CLA. For the second scenario, the number of incident signals is set as $K = 19$, which is bigger than any possible number of physical sensors turned on by RIS CLA, while other parameters remain the same. Simulation results are shown in Figure 5.

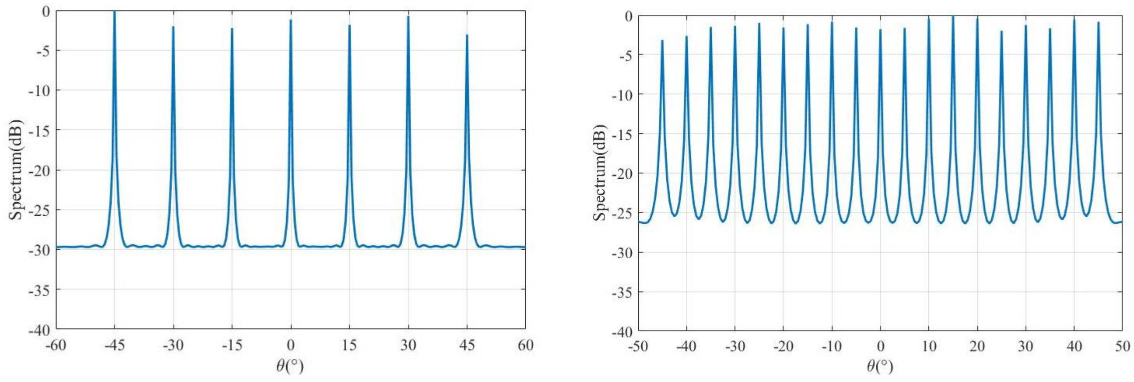

(**a**) (**b**)

Figure 5. Spatial spectrum of the proposed algorithm: (**a**) $K = 7$; (**b**) $K = 19$.

From Figure 5, it is observed that the proposed algorithm is able to distinguish different irrelevant incident signals, even when there are more incident signals than the physical sensors. However, the incident signals given in this simulation are uniformly distributed, which means the minimum difference between incident angles $\Delta\theta$ is 5°, a relatively large value that is not convincing enough. In order to further investigate the effectiveness of our algorithm, the difference of incident angles of certain signals is reduced. Further simulation is performed and the results are shown in Figure 6, with the number of sources $K = 11$. Other simulation parameters remain unchanged.

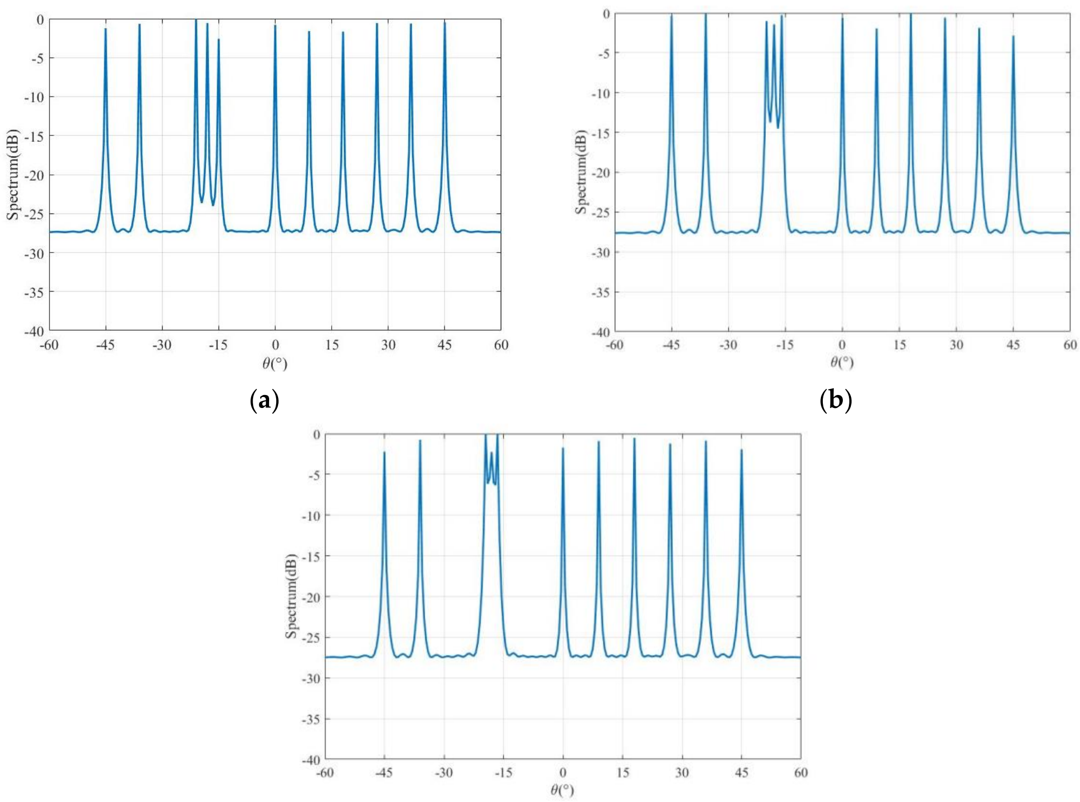

(**c**)

Figure 6. Spectrum of 11 incoherent signals: (**a**) $\Delta\theta$ = 3°; (**b**) $\Delta\theta$ = 2°; (**c**) $\Delta\theta$ = 1.5°.

Results show that the proposed algorithm can effectively distinguish irrelevant signals within a narrow range. Specifically, under the scenario where $\Delta\theta$ = 1.5°, the gap of SNR between the interference and the signal is kept at about 5 dB, which means that adjacent signals are distinguished and that the algorithm is still effective. However, such effectiveness is related to the incident angle of signals. That is, our proposed algorithm is not able to tell apart spatially contiguous signals if their incident signal is more than 60 degrees.

5.3. Resolution Performance

Higher spatial DOF also helps to improve the resolution of DOA estimation algorithms. However, the simulation results in Section 5.2 are not persuasive enough to evaluate the resolution performance of the proposed algorithm. Therefore, root mean square error (RMSE) of angle estimation is introduced as the criterion of resolution to compare different algorithms. The expression of RMSE is given as follows, where M and $\hat{\theta}_{k,m}$ are the cycling index of MCS and estimated value of θ_k during the m-th MCS, respectively.

$$\mathrm{RMSE} = \frac{1}{K}\sum\nolimits_{k=1}^{K}\sqrt{\frac{1}{M}\sum\nolimits_{m=1}^{M}\left(\hat{\theta}_{k,m}-\theta_k\right)^2}\,, \tag{14}$$

To make sure that the performance of the algorithms is compared under a rather fair and reasonable environment, two main irrelevant variables, namely the physical sensors in the array and the total snapshots, should be kept the same for every algorithm. Specifically, it is easy to set the number of these variables for ULA-based algorithms. As for CLA-MUSIC, the number of physical sensors and total snapshots should be the same as in ULA, and the snapshots for each subarray should be the same. For the proposed algorithm we set $N = 30$, so as to match the setting of CLA-MUSIC, and the number of different co-number pairs is set as 3, which is a comprehensive result of complexity and resolution. The number of total snapshots remains the same and is evenly distributed to each subarray. Values of related parameters of the included algorithms are shown in Table 1 and the simulation result is given in Figure 7.

Table 1. Parameters of different DOA estimation algorithms.

Algorithm	Array Parameters	Snapshots
MUSIC [3]	$N = 10$	$J = 900$
w-MUSIC [6]	$N = 10$	$J = 900$
root-MUSIC [4]	$N = 10$	$J = 900$
CLA-MUSIC [14]	2 subarrays with size of 5 and 6	450 for each subarray, 900 in total
Proposed Algorithm	$N = 30$	$t = 3,\ J = 150$ 900 in total

According to Figure 7, DOA estimation algorithms based on CLA and RIS CLA perform better than those based on ULA, primarily thanks to the increased DOF. Furthermore, the proposed algorithm generally performs better than CLA-MUSIC under different SNR. Noticeably, the RMSE of the proposed algorithm is sufficiently good under low SNR, with an improvement more than 75% compared to MUSIC and 25% compared to CLA-MUSIC, respectively. The improvement of DOF provided by the RIS CLA is the main reason why our algorithm has such an advantage. Furthermore, such improvement is proportional to the increase of DOF, which illustrates that the DOF of an array is a decisive factor for the resolution of the DOA algorithm. On the other hand, our proposed method also has some defects as follows: (1) our algorithms work under the assumption that the incident signals are static, which means this method is not applicable if moving targets were to be tracked; (2) compared to other MUSIC-based algorithms, our method requires a rather large number of snapshots. The total number of snapshots is evenly distributed to each subarray, and to guarantee the precision of the received signal of each subarray, the number of snapshots of each subarray should not be too small. Results show that this policy works well. However, it takes more time to finish the signal receiving process, and the time complexity of the algorithm is not outstanding, due to more time in the construction of the difference array.

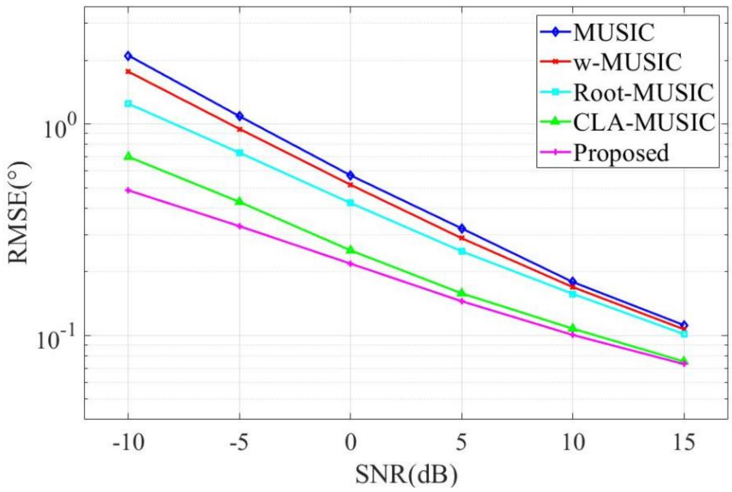

Figure 7. RMSE of different types of MUSIC algorithms.

6. Conclusions & Future Work

Due to the real-time controllability of the RIS array, RIS CLA is capable of constructing CLAs with different combinations and therefore improves DOF. In this paper, we propose, for the very first time, a DOA estimation algorithm of RIS CLA based on MUSIC. Simulation results show that the DOF of RIS CLA improves by more than 30% compared with the traditional CLA. Moreover, the proposed algorithm can effectively tell apart different irrelevant incident signals, even when the number of sources is more than that of the physically deployed sensors. With respect to resolution, the proposed algorithm outperforms the traditional MUSIC algorithm, with an elevation up to 70% and 30% under low SNR compared to MUSIC based on ULA and CLA, respectively. As for future development, an RIS array helps to construct arrays that are instantly controllable. On this basis, sparse arrays based on RIS may be a promising, critical technique for the further development of the intelligent wireless communication network in the field of localization, high-resolution beamforming, wireless channel sensing and so on. Furthermore, it is an important topic to combine RIS technology with array signal processing techniques and take it to another level, focusing on other research topics, such as how to further improve the performance and practicability of existing estimation algorithms. Specifically, further research, such as two-dimensional DOA estimation problem based on RIS array, DOA estimation for coherent signals based on RIS array, derivation of complexity of RIS-array-based estimation algorithm remain to be discussed and conducted. Furthermore, an RIS can be flexibly deployed, so it provides more possibilities not only in the field of wireless communication, but to other related topics such as source location, target tracking and underwater positioning [27].

Author Contributions: Conceptualization, T.L. and L.J.; methodology, T.L. and X.X.; software, T.L.; validation, X.X. and X.S.; formal analysis, T.L. and X.X.; investigation, T.L.,X.S. and X.X.; data curation, T.L. and X.S.; writing—original draft preparation, T.L.; writing—review and editing, K.H. and X.X.; project administration, K.H. and Z.Z.; funding acquisition, K.H. All authors have read and agreed to the published version of the manuscript.

Funding: This research was funded by NSFC (61871404) and CPSF (47725).

Institutional Review Board Statement: Not applicable.

Informed Consent Statement: Not applicable.

Data Availability Statement: Data are contained within the article.

Acknowledgments: We would like to thank Jinghua Qu for writing—review and editing, as well as Zheyuan Deng for his assistance in formal analysis.

Conflicts of Interest: The authors declare no conflict of interest.

References

1. Haykin, S.; Reilly, J.; Kezys, V.; Vertatschitsch, E. Some aspects of array signal processing. *IEE Proc. F Radar Signal Process.* **1992**, *139*, 1–26. [CrossRef]
2. Johnson, D.H.; Dan, E.D. *Array Signal Processing: Concepts and Techniques*, 1st ed.; PTR Prentice Hall: Hoboken, NJ, USA, 1992; pp. 59–106. ISBN 0130485136.
3. Schmidt, R. Multiple emitter location and signal parameter estimation. *IEEE Trans. Antennas Propag.* **1986**, *34*, 276–280. [CrossRef]
4. Rao, B.; Hari, K. Performance Analysis of Root-Music. *IEEE Trans. Acoust. Speech Signal Process.* **1989**, *37*, 1939–1949. [CrossRef]
5. Du, W.; Kirlin, R. Improved spatial smoothing techniques for DOA estimation of coherent signals. *IEEE Trans. Signal Process.* **1991**, *39*, 1208–1210. [CrossRef]
6. Stoica, P.; Nehorai, A. MUSIC, maximum likelihood and Cramer-Rao bound. *IEEE Trans. Acoust. Speech Signal Process.* **1989**, *37*, 720–741. [CrossRef]
7. Berryman, J.G. Maximum entropy spectral analysis. *J. China Inst. Comm.* **2009**, *17*, 1519–1533. [CrossRef]
8. Capon, J. High-resolution frequency-wavenumber spectrum analysis. *Proc. IEEE* **1969**, *57*, 1408–1418. [CrossRef]
9. Roy, R.; Kailath, T. ESPRIT-estimation of signal parameters via rotational invariance techniques. *IEEE Trans. Acoust. Speech Signal Process.* **1989**, *37*, 984–995. [CrossRef]
10. Almidfa, K. Performance analysis of ESPRIT, TLS-ESPRIT and Unitary-ESPRIT algorithms for DOA estimation in a W-CDMA mobile system. In Proceedings of the First International Conference on 3G Mobile Communication Technologies; Institution of Engineering and Technology (IET), London, UK, 27–29 March 2000.
11. Liu, Y.; Hou, L.; Shen, Q.; Lv, C.; Na, S.; Qiu, T. Beamspace U-ESPRIT DOA Estimation Algorithm of Coherently Distributed Sources in Massive MIMO Systems. In Proceedings of the 2020 12th International Conference on Advanced Computational Intelligence (ICACI), Dali, China, 14–16 August 2020; pp. 126–132. [CrossRef]
12. Krim, H.; Viberg, M. Two decades of array signal processing research: The parametric approach. *IEEE Signal Process. Mag.* **1996**, *13*, 67–94. [CrossRef]
13. Vaidyanathan, P.P.; Pal, P. Sparse Sensing with Co-Prime Samplers and Arrays. *IEEE Trans. Signal Process.* **2011**, *59*, 573–586. [CrossRef]
14. Pal, P.; Vaidyanathan, P.P. Coprime Sampling and the Music Algorithm. In Proceedings of the 14th IEEE Digital Signal Processing Workshop and IEEE Signal Processing Education Workshop, Sedona, AZ, USA, 4–7 January 2011. [CrossRef]
15. Qin, S.; Zhang, Y.D.; Amin, M.G. Generalized Coprime Array Configurations for Direction-of-Arrival Estimation. *IEEE Trans. Signal Process.* **2015**, *63*, 1377–1390. [CrossRef]
16. Jia, Y.; Li, Z.; Yan, C.; Duo, B.; Zhong, X.; Guo, Y.; Yin, S. DOA Estimation for Coherent and Incoherent Sources Based on Co-Prime Array. In Proceedings of the 10th EAI International Conference on Wireless and Satellite Systems, Harbin, China, 12–13 January 2019; pp. 608–619. [CrossRef]
17. Dong, X.; Sun, M.; Zhang, X.; Zhao, J. Fractional Low-Order Moments Based DOA Estimation with Co-Prime Array in Presence of Impulsive Noise. *IEEE Access* **2021**, *9*, 23537–23543. [CrossRef]
18. Wan, Z.; Liu, W. Non-Coherent DOA Estimation via Proximal Gradient Based on a Dual-Array Structure. *IEEE Access* **2021**, *9*, 26792–26801. [CrossRef]
19. Ashok, C.; Venkateswaran, N. Manifold Ambiguity-Free Low Complexity DOA Estimation Method for Unfolded Co-Prime Arrays. *IEEE Commun. Lett.* **2021**, *25*, 1886–1890. [CrossRef]
20. Wu, Q.; Zhang, S.; Zheng, B.; You, C.; Zhang, R. Intelligent Reflecting Surface-Aided Wireless Communications: A Tutorial. *IEEE Trans. Commun.* **2021**, *69*, 3313–3351. [CrossRef]
21. Wu, Q.; Zhang, R. Towards Smart and Reconfigurable Environment: Intelligent Reflecting Surface Aided Wireless Network. *IEEE Commun. Mag.* **2020**, *58*, 106–112. [CrossRef]
22. Tang, W.; Chen, M.Z.; Chen, X.; Dai, J.Y.; Han, Y.; Di Renzo, M.; Zeng, Y.; Jin, S.; Cheng, Q.; Cui, T.J. Wireless Communications with Reconfigurable Intelligent Surface: Path Loss Modeling and Experimental Measurement. *IEEE Trans. Wirel. Commun.* **2021**, *20*, 421–439. [CrossRef]
23. Yu, N.; Genevet, P.; Kats, M.A.; Aieta, F.; Tetienne, J.-P.; Capasso, F.; Gaburro, Z. Light Propagation with Phase Discontinuities: Generalized Laws of Reflection and Refraction. *Science* **2011**, *334*, 333–337. [CrossRef]
24. Cui, T.J.; Qi, M.Q.; Wan, X.; Zhao, J.; Cheng, Q. Coding metamaterials, digital metamaterials and programmable metamaterials. *Light. Sci. Appl.* **2014**, *3*, e218. [CrossRef]
25. Dai, L.; Wang, B.; Wang, M.; Yang, X.; Tan, J.; Bi, S.; Xu, S.; Yang, F.; Chen, Z.; Di Renzo, M.; et al. Reconfigurable Intelligent Surface-Based Wireless Communications: Antenna Design, Prototyping, and Experimental Results. *IEEE Access* **2020**, *8*, 45913–45923. [CrossRef]

26. Nyquist, H. Certain topics in telegraph transmission theory. *Trans. AIEE.* **1928**, *47*, 617–644. [CrossRef]
27. Dey, N.; Ashour, A.S.; Shi, F.; Sherratt, R.S. Wireless Capsule Gastrointestinal Endoscopy: Direction-of-Arrival Estimation Based Localization Survey. *IEEE Rev. Biomed. Eng.* **2017**, *10*, 2–11. [CrossRef] [PubMed]